JACS
JOURNAL OF THE AMERICAN CHEMICAL SOCIETY
Communication
pubs.acs.org/JACS

Electrocatalytic Water Oxidation with a Copper(II) Polypeptide Complex

Ming-Tian Zhang, Zuofeng Chen, Peng Kang, and Thomas J. Meyer*

Department of Chemistry, University of North Carolina at Chapel Hill, Chapel Hill, North Carolina 27599, United States

Supporting Information

ABSTRACT: A self-assembly-formed triglycylglycine macrocyclic ligand (TGG^{4-}) complex of Cu(II), $[(TGG^{4-})Cu^{II}-OH_2]^{2-}$, efficiently catalyzes water oxidation in a phosphate buffer at pH 11 at room temperature by a well-defined mechanism. In the mechanism, initial oxidation to Cu(III) is followed by further oxidation to a formal "Cu(IV)" with formation of a peroxide intermediate, which undergoes further oxidation to release oxygen and close the catalytic cycle. The catalyst exhibits high stability and activity toward water oxidation under these conditions with a high turnover frequency of 33 s^{-1}.

Catalytic water oxidation is an active area of research, of fundamental interest because of its importance in natural and artificial photosynthesis as the "other half reaction".[1] Notable progress has been made in homogeneous water oxidation catalysis with transition metal complexes, including mononuclear, binuclear, and multinuclear complexes of manganese,[2] ruthenium,[3] iridium,[4] iron,[5] and cobalt.[6] Limitations arise from the use of precious metals involved catalysts, strenuous catalyst synthesis, or unstable catalysts under the conditions needed for sustained catalysis. In integrated chromophore–catalyst assemblies for solar fuel applications, an additional complication arises if the catalyst is a competitive, nonproductive light absorber. These factors emphasize the importance of identifying efficient, robust first-row molecular catalysts with low light absorptivites.

Copper is an earth-abundant and biorelevant metal, yet the use of Cu for water oxidation is much less explored. In an earlier report, Mayer and co-workers reported on a Cu(II) 2,2′-bipyridine catalyst for water oxidation.[7] We report here a well-defined Cu(II) complex prepared *in situ* from a triglycylglycine macrocyclic ligand, $[(TGG^{4-})Cu^{II}-OH_2]^{2-}$, Figure 1, which is an efficient, rapid electrocatalyst for water oxidation undergoing multiple turnovers with retention of its catalytic reactivity. Mechanistically, the results of electrochemical studies reveal a stable Cu^{III} form and experimental details that point to the mechanism of water oxidation.

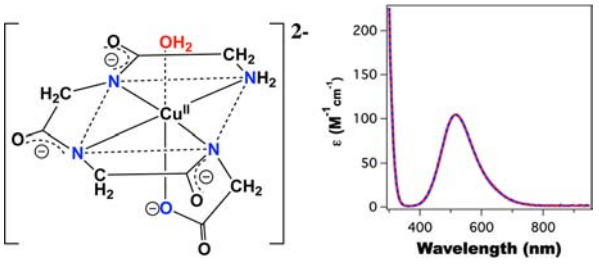

Figure 1. (Left) Structure of the catalyst, $[(TGG^{4-})Cu^{II}-OH_2]^{2-}$. (Right) Its absorption spectrum in 0.25 M phosphate buffer at pH 11.

Catalyst Structure. The coordination of Cu in metalloproteins and synthetic forms has been extensively investigated.[8] The structure of the Cu(II) complex of the triglycylglycine macrocyclic ligand in Figure 1 at high pH was reported previously.[8b,9] The coordination between Cu^{II} and the triglycylglycine macrocyclic ligand is pH dependent, with the pH dependence arising from the amide groups with successively increasing pK_a values (5.6, 6.8, 9.0); the deprotonated structure shown in Figure 1 dominates at pH >10.[8b,9] The catalyst was independently synthesized as described in the literature, and its absorption spectrum (blue line, Figure 1) is the same as for the self-assembled complex in solution when the ligand and $Cu(OH)_2$ were mixed in a 1:1 ratio at pH 11 (red dashed line in Figure 1). The complex has a characteristic d-d absorption at 530 nm with molar absorptivity of $\varepsilon_{max} \approx 100\ M^{-1}\ cm^{-1}$.

Cyclic Voltammetry (CV). The redox properties of the complex were investigated by CV in water with added phosphate buffers. The CVs were recorded in air at glassy carbon (GC), boron-doped diamond (BDD), and tin-doped indium oxide (ITO) working electrodes. The reference electrode was a saturated calomel electrode with potentials reported vs normal hydrogen electrode (NHE) by the addition of 0.244 V to measured potentials. Figure 2 shows CVs of $[(TGG^{4-})Cu^{II}-OH_2]^{2-}$ obtained at pH 11 in a 0.25 M phosphate buffer solution at a GC working electrode.

In the CV, one well-defined, reversible oxidation wave appears at $E_{1/2}$ = +0.58 V vs NHE with a peak-to-peak splitting of ΔE_p = 70 mV at a scan rate of 10 mV/s. This wave is pH dependent, decreasing by ~59 mV/pH (Figures S1–S3). The pH dependence is consistent with reversible oxidation of the Cu(II) form of $[(TGG^{4-})Cu^{II}-OH_2]^{2-}$ to Cu(III) by proton-coupled electron transfer to give the hydroxyl form, with the couple shown in eq 1.[10]

$$[(TGG^{4-})Cu^{II}-OH_2]^{2-} \xrightarrow{-e^-,-H^+} [(TGG^{4-})Cu^{III}-OH]^{2-} \quad (1)$$

At more positive potentials, an additional, irreversible oxidation wave appears at $E_{p,a}$ = 1.32 V vs NHE in 0.25 M phosphate buffer (pH 11) with a greatly enhanced underlying

Received: October 4, 2012
Published: January 27, 2013

dx.doi.org/10.1021/ja3097515 | J. Am. Chem. Soc. 2013, 135, 2048–2051

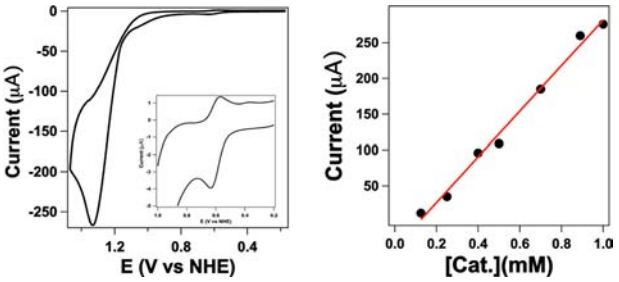

Figure 2. (Left) CV in 0.25 M phosphate buffer (pH 11) at a GC electrode, 0.89 mM $[(TGG^{4-})Cu^{II}-OH_2]^{2-}$, scan rate = 10 mV/s. The inset shows a magnified view of the $Cu^{III/II}$ couple at $E_{1/2}$ = 0.58 V. (Right) Plot of catalytic peak current at $E_{p,a}$ = 1.32 V vs the concentration of catalyst.

current compared to the background.[11] As shown in the CV, on a reverse scan, the reversible wave for the $[(TGG^{4-})Cu^{III}-OH]^{2-}/[(TGG^{4-})Cu^{II}-OH_2]^{2-}$ couple is observed without loss of peak current, consistent with water oxidation catalysis rather than oxidative decomposition of the complex. The current enhancement for the wave at $E_{p,a}$ = 1.32 V is consistent with catalytic water oxidation. The onset for water oxidation appears at ~1.10 V vs NHE, an overpotential of ~0.52 V. Water oxidation is due to the complex and not from uncomplexed Cu(II) in solution. Addition of 1 mM $CuSO_4$ to the 0.25 M phosphate buffer (pH 11) resulted in immediate precipitation of $Cu_3(PO_4)_2$ ($K_{p,a} = 1.40 \times 10^{-37}$) and/or $Cu(OH)_2$ ($K_{p,a} = 2.0 \times 10^{-19}$), and the resulting solution/suspension has no activity toward water activation (Figure S4).[12]

Electrocatalytic Water Oxidation by $[(TGG^{4-})Cu^{II}-OH_2]^{2-}$. Evolution of O_2 as a product was investigated by controlled potential electrolysis at +1.3 V on a large surface area ITO (0.70 cm^2) electrode with 2 mM $[(TGG^{4-})Cu^{II}-OH_2]^{2-}$ in 0.25 M phosphate buffer (pH 11) (Figure 3, left, and Figure

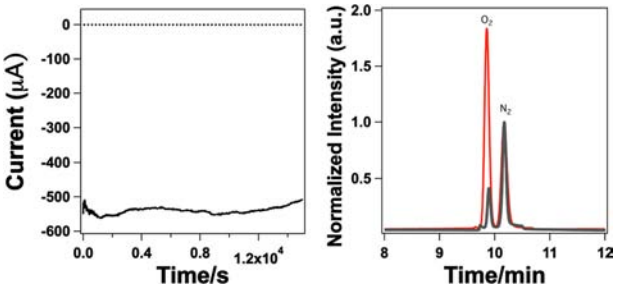

Figure 3. (Left) Catalytic current obtained upon controlled potential electrolysis without (dashed line) and with (solid line) 1 mM $[(TGG^{4-})Cu^{II}-OH_2]^{4-}$ at an ITO electrode (0.70 cm^2) in 0.25 M phosphate buffer (pH 11) at 1.30 V vs NHE. (Right) Normalized gas chromatographic trace before (black line) and after (red line) electrolysis.

S5). The background for oxygen formation at the applied potential in the absence of catalyst was negligibly small. With added $[(TGG^{4-})Cu^{II}-OH_2]^{2-}$, the catalytic current was sustained for at least ~5 h at a stable current density of 0.80 mA/cm^2. After a 5 h electrolysis period, the current slightly decreased due the decrease in pH by 1.5 units, consistent with consumption of OH^- by water oxidation,[13] $4OH^- \xrightarrow{4e^-} O_2 + 2H_2O$.The original catalytic current density was recovered when the solution pH was adjusted back to the original 11, and was then sustained for an additional 5 h.

The evolved O_2 was analyzed by gas chromatography (Varian 450-GC), Figure 3 (right), which gave ~39 μmol of O_2 over an electrolysis period of 8 h with a Faradaic efficiency of 99% for O_2 through ~13 catalytic turnovers based on the initial amount of $[(TGG^{4-})Cu^{II}-OH_2]^{2-}$ in the solution.

Water oxidation catalysis is homogeneous. Following long-term electrolysis, and up to 13 turnovers, there was no spectroscopic change in the electrolysis solution when the solution pH was adjusted back to 11, showing that the catalyst was intact. There was no evidence for heterogeneity of the catalyst. Over multiple CVs and during controlled potential electrolysis, there were insignificant changes in peak currents or wave shape (Figure S6). A GC electrode subjected to catalytic water oxidation electrolysis at 1.32 V vs NHE with ~1 mM $[(TGG^{4-})Cu^{II}-OH_2]^{2-}$ at pH 11 for 2 h gave no catalytic response in a fresh, copper-catalyst-free electrolyte at pH 11 (Figure S7). Under the same conditions, but at an ITO electrode, there was no evidence for precipitation or film formation by absorption spectrum (Figure S8), SEM (Figure S9), and XPS (Figure S10) after a 2 h electrolysis period.

Kinetics. The catalytic peak current for water oxidation, i_{cat}, varies linearly with the concentration of catalyst, $[(TGG^{4-})Cu^{II}-OH_2^{2-}]$ (Figure 2), consistent with single-site copper catalysis and eq 2,[14]

$$i_{cat} = n_{cat}FA[Cu](k_{cat}D_{Cu})^{1/2} \quad (2)$$

where n_{cat} = 4 is the electrochemical stoichiometry for water oxidation, F is the Faraday constant, A is the electrode surface area (in cm^2), [Cu] is the concentration of catalyst (in mol/L), and D_{Cu} is the diffusion coefficient of the catalyst in 0.25 M phosphate buffer at pH 11. As shown in Figure 4, and as

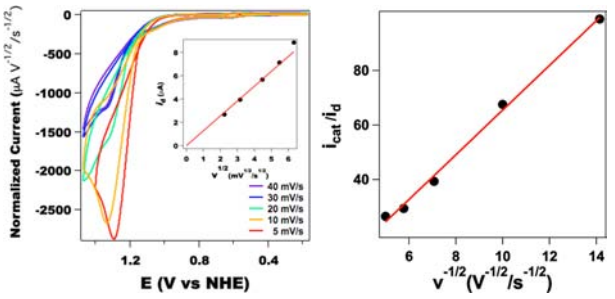

Figure 4. (Left) Normalized CVs ($i/v^{1/2}$) for 0.89 mM $[(TGG^{4-})Cu^{II}-OH_2]^{2-}$ in 0.25 M phosphate buffer at pH 11 at different scan rates (v) (GC working electrode). Inset: Dependence of the peak current for the Cu(III/II) couple at $E_{p,a}$ = 0.58 V vs $v^{1/2}$. (Right) Plot of the ratio of the catalytic current at 1.32 V, i_{cat}, to the oxidative peak current for the Cu(III/II) wave, i_d, vs $v^{-1/2}$; see text.

expected for a solution couple, the peak current for the Cu(III/II) couple under these conditions at +0.58 V vs NHE varies linearly with the square root of the scan rate ($v^{1/2}$), Figure 4. This result is consistent with the Randles–Sevcik equation,

$$i_d = 0.4633nFA[Cu](nFvD_{Cu}/RT)^{1/2} \quad (3)$$

with T the absolute temperature and n = 1, the number of electrons transferred for the Cu(III/II) couple. From the slope of the line, $D_{Cu} \approx 1 \times 10^{-5}$ cm^2/s. The ratio of eqs 2 and 3 gives eq 4,

$$i_{cat}/i_d = 2.242(k_{cat}RT/Fv)^{1/2} \quad (4)$$

dx.doi.org/10.1021/ja3097515 | J. Am. Chem. Soc. 2013, 135, 2048–2051

From the slope of the plot of the ratio, i_{cat}/i_d vs $\nu^{-1/2}$ in Figure 4, k_{cat} = 33 s^{-1} in 0.25 M phosphate buffer at pH 11 at room temperature.[14] In fact, this value may be a lower limit. As noted by a reviewer, the catalytic wave may be influenced by local depletion effects decreasing the pH and changing the buffer ratio, although these effects should be mitigated by the high buffer concentrations used.

For water oxidation, with water as the substrate, the measured value of k_{cat} is also the catalytic turnover frequency for catalytic water oxidation. The value here is comparable with that of the previously reported copper bipyridine catalyst under comparable conditions but at higher pH (~100 s^{-1} at pH 13).[7]

Mechanism. Based on the results of mechanistic studies, largely on Ru[15] and Ir[4a,b] complexes, the key O−O bond-forming step in water oxidation appears to occur by either O-atom transfer to a water molecule, with coupled proton loss to an added base or second water molecule,[15] or intramolecular O−O coupling.[3d]

With $[(TGG^{4-})Cu^{II}-OH_2]^{2-}$ as the catalyst, initial oxidation to $[(TGG^{4-})Cu^{III}-OH]^{2-}$ is followed by a second irreversible oxidation. The second oxidation occurs by a well-defined, catalytically enhanced diffusional wave that appears at $E_{p,a}$ = 1.32 V vs NHE in 0.25 M phosphate buffer at pH 11. This wave also varies linearly with [Cu]. The current density for this wave is greatly enhanced by an underlying, potential-dependent catalytic current for water oxidation. The peak potential for the second wave is also pH dependent, varying by ~ −150 mV/pH unit, with the true pH dependence presumably distorted by the underlying catalytic process (Figure S11).

Based on these observations, a mechanism for water oxidation is proposed in eqs 5−7 and Scheme 1. In this mechanism, the wave at $E_{p,a}$ = 1.32 V vs NHE arises from further oxidation of $[(TGG^{4-})Cu^{III}-OH]^{2-}$, with the pH dependence suggesting additional proton loss. The product of the second oxidation would be the formally d^7 $[(TGG^{4-})Cu^{IV}(O)]^{2-}$ intermediate shown in eq 5,

$$[(TGG^{4-})Cu^{III}-OH]^{2-} \xrightarrow{-e^-,-H^+} [(TGG^{4-})Cu^{IV}(O)]^{2-} \quad (5)$$

It is analogous to the reactive d^3 $Ru^{V}(O)$ form of Ru polypyridyl complexes[15b] and, presumably, largely ligand-centered oxyl in character, i.e., $[(TGG^{4-})Cu^{III}(O^{\bullet})]^{2-}$.[16]

Scheme 1. Proposed Mechanism for Water Oxidation by $[(TGG^{4-})Cu^{II}-OH_2]^{2-}$ in Phosphate Buffer Solutions at pH 11[a]

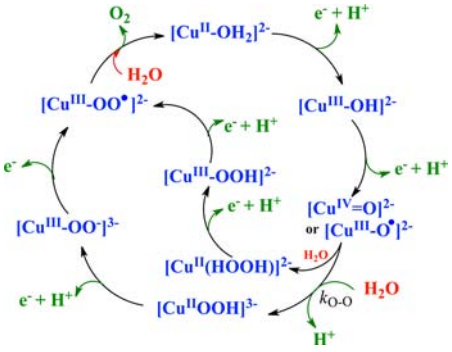

[a]In the catalytic cycle, electrochemical evidence has been obtained for $[Cu^{III}-OH]^{2-}$, $[Cu^{IV}(O)]^{2-}$, $[Cu^{II}-OOH]^{3-}$ or $[Cu^{II}(HOOH)]^{2-}$, and $[Cu^{III}-OO^{-}]^{3-}$ or $[Cu^{III}-OOH]^{2-}$.

In the mechanism in Scheme 1, once formed, the $Cu^{IV}(O)$ intermediate undergoes rate-limiting O−O bond formation by reaction with water, eq 6a.

$$[(TGG^{4-})Cu^{IV}(O)]^{2-} + H_2O \rightarrow [(TGG^{4-})Cu^{II}(HOOH)]^{2-} \quad (6a)$$

$$[(TGG^{4-})Cu^{IV}(O)]^{2-} + H_2O + B \rightarrow [(TGG^{4-})Cu^{II}(OOH)]^{3-} + H-B^{+} \quad (6b)$$

As found for $[Ru^{V}(tpy)(bpm)(O)]^{3+}$ (tpy = 2,2′;6′,2″-terpyridine; bpm = 2,2′-bipyrimidine) and shown in eq 6b, oxo transfer may involve a second water molecule or added base—OH^-, HPO_4^{2-}, PO_4^{3-}—as a proton acceptor and atom-proton transfer (APT)[15b] to give a hydroperoxide intermediate ($Cu^{II}(OOH)$) directly. The catalytic peak current for the wave at 1.32 V vs NHE, normalized by the square root of the scan rate ($i_{p,a}/\nu^{1/2}$), Figure 4, increases with decreasing scan rate, consistent with a chemical step and rate-limiting O−O bond formation. With this interpretation, k_{cat} obtained from the rate studies is the rate constant for the O−O bond-forming step in eqs 6a and 6b. The catalytic peak current is dependent on the concentration of buffer base, HPO_4^{2-} + PO_4^{3-}, at fixed pH (Figures S12 and S13), pointing to a contribution from an APT pathway and the reaction in eq 6b.

The irreversibility for the second oxidation, and the elevated current levels following oxidation to $[(TGG^{4-})Cu^{IV}(O)]^{2-}$, presumably come from further oxidation of the intermediate peroxide, release of O_2, and re-entry into the catalytic cycle, Scheme 1 and eq 7 or their equivalents, followed by further oxidation of $[(TGG^{4-})Cu^{II}(OOH)]^{3-}$. This mechanism is analogous to the mechanism established for single-site Ru polypyridyl water oxidation catalysts.[15]

$$[(TGG^{4-})Cu^{II}(OOH)]^{3-} \xrightarrow{-4e^-,-3H^+,+H_2O} [(TGG^{4-})Cu^{IV}{=}O]^{2-} + O_2 \quad (7)$$

As shown in Figure 5, there is evidence for the proposed peroxide intermediate in CVs. Following an oxidative scan through the catalytic wave at $E_{p,a}$ ≈ 1.3 V (pH 11 at a scan rate of 100 mV/s), a new wave appears at $E_{1/2}$ = 0.38 V (Figure 5, black line, and Figure 2 inset). This wave does not appear in

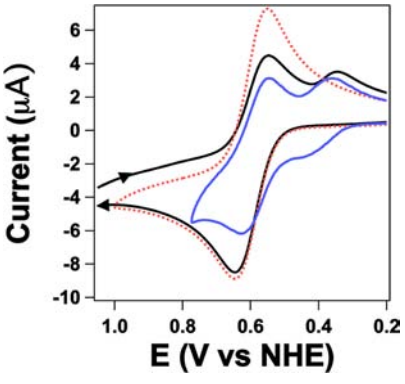

Figure 5. CVs of $[(TGG^{4-})Cu^{II}-OH_2]^{2-}$. (a) Red dashed line: With scan reversal before the catalytic water oxidation wave with the $[(TGG^{4-})Cu^{III}-OH]^{2-}/[(TGG^{4-})Cu^{II}-OH_2]^{2-}$ couple appearing at $E_{1/2}$ = 0.58 V. (b) Black line: With scan reversal following a scan into the catalytic water oxidation wave with the appearance of a new wave at $E_{1/2}$ = 0.38 V. (c) Blue line: After addition of a few drops of dilute H_2O_2. BDD working electrode, at 100 mV/s.

dx.doi.org/10.1021/ja3097515 | J. Am. Chem. Soc. 2013, 135, 2048−2051

CV scans that are reversed before the wave at 1.3 V and only appears at relatively rapid scan rates. Similar observations have been made for polypyridyl Ru complexes and attributed to peroxide intermediates.[15c] We tentatively assign this wave to a peroxide couple, $[(TGG^{4-})Cu^{III}(OO)]^{3-}/[(TGG^{4-})Cu^{II}-OOH]^{3-}$ or $[(TGG^{4-})Cu^{III}(OOH)]^{2-}/[(TGG^{4-})Cu^{II}(HOOH)]^{2-}$. The wave at 0.38 V also appears upon addition of hydrogen peroxide to solutions containing $[(TGG^{4-})Cu^{II}-OH_2]^{2-}$, presumably by substitution of water by peroxide in the aqua complex, $[(TGG^{4-})Cu^{II}-OH_2]^{2-}$ + HOOH → $[(TGG^{4-})Cu^{II}(HOOH)]^{2-}$ + H_2O. Copper peroxo complexes are known as key intermediates in oxygen reduction by copper proteins and synthetic models.[17]

Concluding Remarks. We describe here a robust, reactive, water-soluble Cu(II) catalyst which carries out water oxidation by a well-defined mechanism with key intermediates characterized. The catalyst employs an earth-abundant metal and is easy to prepare based on a polypeptide ligand structure. Although water oxidation occurs at an overpotential of ~0.52 V at pH 11 in 0.25 M phosphate buffer, the rates, turnover numbers, and catalyst stability are impressive.

The stabilities of the catalyst and its peptide ligand system are notable, as well as the ease of synthesis. Given the synthetic versatility of these complexes, a door may be open for the systematic investigation of a large number of related complexes for water oxidation catalysis.

■ ASSOCIATED CONTENT

Ⓢ Supporting Information

Additional information as noted in the text. This material is available free of charge via the Internet at http://pubs.acs.org.

■ AUTHOR INFORMATION

Corresponding Author

tjmeyer@unc.edu

Notes

The authors declare no competing financial interest.

■ ACKNOWLEDGMENTS

This work was supported by the National Science Foundation, award no. NSF 957215. Funding from the U.S. Army Research Office, through Grant W911NF-09-1-0426, and from the UNC EFRC: Solar Fuels and Next Generation Photovoltaics, an Energy Frontier Research Center, funded by U.S. DOE-BES, under award DE-SC0001011, is gratefully acknowledged.

■ REFERENCES

(1) (a) Eisenberg, R.; Gray, H. B. *Inorg. Chem.* **2008**, *47*, 1697. (b) Hurst, J. K. *Science* **2010**, *328*, 315. (c) Meyer, T. J. *Nat. Chem.* **2011**, *3*, 757. (d) Hammarström, L.; Styring, S. *Nat. Chem.* **2009**, *1*, 185. (d) Gagliardi, C. J.; Vannucci, A. K.; Concepcion, J. J.; Chen, Z.; Meyer, T. J. *Energy Environ. Sci.* **2012**, *5*, 7704. (e) Liu, X.; Wang, F. Y. *Coord. Chem. Rev.* **2012**, *256*, 1115.

(2) (a) Ashmawy, F. M.; McAuliffe, C. A.; Parish, R. V.; Tames, J. *J. Chem. Soc., Dalton Trans.* **1985**, 1391. (b) Watkinson, M.; Whiting, A.; McAuliffe, C. A. *J. Chem. Soc., Chem. Comm.* **1994**, 2141. (c) Limburg, J.; Vrettos, J. S.; Liable-Sands, L. M.; Rheingold, A. L.; Crabtree, R. H.; Brudvig, G. W. *Science* **1999**, *283*, 1524. (d) Gao, Y.; Åkermark, T.; Liu, J.; Sun, L.; Åkermark, B. *J. Am. Chem. Soc.* **2009**, *131*, 8726.

(3) (a) Concepcion, J. J.; Jurss, J. W.; Brennaman, M. K.; Hoertz, P. G.; Patrocinio, A. O. T.; Iha, N. Y. M.; Templeton, J. L.; Meyer, T. J. *Acc. Chem. Res.* **2009**, *42*, 1954. (b) Liu, F.; Concepcion, J. J.; Jurss, J. W.; Cardolaccia, T.; Templeton, J. L.; Meyer, T. J. *Inorg. Chem.* **2008**, *47*, 1727. (c) Alstrum-Acevedo, J. H.; Brennaman, M. K.; Meyer, T. J. *Inorg. Chem.* **2005**, *44*, 6802. (d) Duan, L. L.; Bozoglian, F.; Mandal, S.; Stewart, B.; Privalov, T.; Llobet, A.; Sun, L. C. *Nat. Chem.* **2012**, *4*, 418. (e) Romain, S.; Vigara, L.; Llobet, A. *Acc. Chem. Res.* **2009**, *42*, 1944.

(4) (a) Hull, J. F.; Balcells, D.; Blakemore, J. D.; Incarvito, C. D.; Eisenstein, O.; Brudvig, G. W.; Crabtree, R. H. *J. Am. Chem. Soc.* **2009**, *131*, 8730. (b) Blakemore, J. D.; Schley, N. D.; Balcells, D.; Hull, J. F.; Olack, G. W.; Incarvito, C. D.; Eisenstein, O.; Brudvig, G. W.; Crabtree, R. H. *J. Am. Chem. Soc.* **2010**, *132*, 16017. (c) Schley, N. D.; Blakemore, J. D.; Subbaiyan, N. K.; Incarvito, C. D.; D'Souza, F.; Crabtree, R. H.; Brudvig, G. W. *J. Am. Chem. Soc.* **2011**, *133*, 10473.

(5) (a) Ellis, W. C.; McDaniel, N. D.; Bernhard, S.; Collins, T. J. *J. Am. Chem. Soc.* **2010**, *132*, 10990. (b) Fillol, J. L.; Codola, Z.; Garcia-Bosch, I.; Gomez, L.; Pla, J. J.; Costas, M. *Nat. Chem.* **2011**, *3*, 807.

(6) (a) Kanan, M. W.; Nocera, D. G. *Science* **2008**, *321*, 1072. (b) Dogutan, D. K.; McGuire, R.; Nocera, D. G. *J. Am. Chem. Soc.* **2011**, *133*, 9178. (c) Wasylenko, D. J.; Ganesamoorthy, C.; Borau-Garcia, J.; Berlinguette, C. P. *Chem. Commun.* **2011**, *47*, 4249.

(7) Barnett, S. M.; Goldberg, K. I.; Mayer, J. M. *Nat. Chem.* **2012**, *4*, 498.

(8) (a) Cooper, T.; Freeman, H. C.; Schoone, J. C.; Robinson, G. *Nature* **1962**, *194*, 1237. (b) Kim, M. K.; Martell, A. E. *J. Am. Chem. Soc.* **1966**, *88*, 914. (c) Hanaki, A.; Kawashima, T.; Konishi, T.; Takano, T.; Mabuchi, D.; Odani, A.; Yamauchi, O. *J. Inorg. Biochem.* **1999**, *77*, 147. (d) Sovago, I.; Sanna, D.; Dessi, A.; Varnagy, K.; Micera, G. *J. Inorg. Biochem.* **1996**, *63*, 99. (e) Brookes, G.; Pettit, L. D. *J. Chem. Soc., Dalton Trans.* **1975**, 2106. (f) Martin, R. P.; Mosoni, L.; Sarkar, B. *J. Biol. Chem.* **1971**, *246*, 5944. (g) Solomon, E. I.; Chen, P.; Metz, M.; Lee, S.-K.; Palmer, A. E. *Angew. Chem., Int. Ed.* **2001**, *40*, 4570.

(9) Nagy, N. V.; Szabo-Planka, T.; Rockenbauer, A.; Peintler, G.; Nagypal, I.; Korecz, L. *J. Am. Chem. Soc.* **2003**, *125*, 5227.

(10) (a) Margerum, D. W.; Chellappa, K. L.; Bossu, F. P.; Burce, G. L. *J. Am. Chem. Soc.* **1975**, *97*, 6894. (b) Rybka, J. S.; Kurtz, J. L.; Neubecker, T. A.; Margerum, D. W. *Inorg. Chem.* **1980**, *19*, 2791. (c) Bossu, F. P.; Chellappa, K. L.; Margerum, D. W. *J. Am. Chem. Soc.* **1977**, *99*, 2195.

(11) As can be seen in Figure 2, an additional, concentration-dependent feature appears at $E_{p,a} \approx 1.0$ V, but only at high concentrations of the catalyst. This feature is currently under investigation and may arise from an additional, di-Cu pathway.

(12) Chen, Z.; Meyer, T. J. *Angew. Chem., Int. Ed.* **2013**, *52*, 700.

(13) This pH decrease is due to slow H^+ equilibrium through the frit which separates the Pt counter electrode from the working compartment solution.

(14) Bard, A. J.; Faulkner, L. R. *Electrochemical methods: Fundamentals and Applications*; Wiley: New York, 2001.

(15) (a) Yang, X. Z.; Hall, M. B. *J. Am. Chem. Soc.* **2010**, *132*, 120. (b) Chen, Z. F.; Concepcion, J. J.; Hu, X. Q.; Yang, W. T.; Hoertz, P. G.; Meyer, T. J. *Proc. Natl. Acad. Sci. U.S.A.* **2010**, *107*, 7225. (c) Chen, Z.; Concepcion, J. J.; Luo, H.; Hull, J. F.; Paul, A.; Meyer, T. J. *J. Am. Chem. Soc.* **2010**, *132*, 17670. (d) Wang, L. P.; Wu, Q.; Van Voorhis, T. *Inorg. Chem.* **2010**, *49*, 4543. (e) Concepcion, J. J.; Tsai, M. K.; Muckerman, J. T.; Meyer, T. J. *J. Am. Chem. Soc.* **2010**, *132*, 1545.

(16) Winkler, J. R.; Gray, H. B. *Struct. Bonding (Berlin)* **2012**, *142*, 17.

(17) (a) Fukuzumi, S.; Kotani, H.; Lucas, H. R.; Doi, K.; Suenobu, T.; Peterson, R. L.; Karlin, K. D. *J. Am. Chem. Soc.* **2010**, *132*, 6874. (b) Fukuzumi, S.; Tahsini, L.; Lee, Y.-M.; Ohkubo, K.; Nam, W.; Karlin, K. D. *J. Am. Chem. Soc.* **2010**, *134*, 7025. (c) McCrory, C. C.; Devadoss, A.; Ottenwaelder, X.; Lowe, R. D.; Stack, D. P.; Chidsey, C. E. D. *J. Am. Chem. Soc.* **2011**, *133*, 3696.